Journal of Alzheimer's Disease 21 (2010) 915–926
DOI 10.3233/JAD-2010-100471
IOS Press

Amyloid-β_{25-35}, an Amyloid-β_{1-42} Surrogate, and Proinflammatory Cytokines Stimulate VEGF-A Secretion by Cultured, Early Passage, Normoxic Adult Human Cerebral Astrocytes

Anna Chiarini[a], James Whitfield[b], Clara Bonafini[a], Balu Chakravarthy[b], Ubaldo Armato[a,*] and Ilaria Dal Prà[a]

[a]*Histology and Embryology Unit, Department of Life and Reproduction Sciences, University of Verona Medical School, Verona, Italy*

[b]*Molecular Signalling Group, National Research Council of Canada, Institute for Biological Sciences, Ottawa, ON, Canada*

Accepted 21 April 2010

Abstract. Cerebrovascular angiopathy affects late-onset Alzheimer's disease (LOAD) brains by possibly increasing vascular endothelial growth factor (VEGF). A expression, thereby stimulating endothelial cell proliferation and migration. Indeed, *VEGF-A* gene upregulation, with increased VEGF-A protein content of reactive astrocytes and microglia, occurs in LOAD brains, and neovascularization was observed one week after injecting amyloid-β (Aβ)$_{1-42}$ into rat hippocampus. We have now found, with cultured 'normoxic' normal adult human astrocytes (NAHAs), that fibrillar Aβ_{25-35} (an active Aβ_{1-42} fragment) or a cytokine mixture (the (CM)-trio (interleukin [IL]-1β+interferon [IFN]-γ+tumor necrosis factor [TNF]-α), or pair (IFN-γ+TNF-α) like those produced in LOAD brains) stimulates the nuclear translocation of stabilized hypoxia-inducible factor (HIF)-1α protein and its binding to *VEGF-A* hypoxia-response elements; the mRNA synthesis for three VEGF-A splice variants (121, 165, 189); and the secretion of VEGF-A$_{165}$. The CM-trio was the most powerful stimulus, IFN-γ+TNF-α was less potent, and other cytokine pairs or single cytokines or Aβ_{35-25} were ineffective. While Aβ_{25-35} did not change HIF-1β protein levels, the CM-trio increased both HIF-1α and HIF-1β protein levels, thereby giving an earlier and stronger stimulus to VEGF-A secretion by NAHAs. Thus, increased VEGF-A secretion from astrocytes stimulated by Aβ_{1-42} and by microglia-released cytokines might restore angiogenesis and Aβ_{1-42} vascular clearance.

Keywords: Alzheimer's disease, amyloid-β peptides, cerebrovascular angiopathy, HIF-1, normal adult human astrocytes, proinflammatory cytokines, VEGF-A

INTRODUCTION

VEGF (vascular endothelial growth factor) is best known as a hypoxia-inducible, secreted protein that activates receptor protein tyrosine kinases on vascular endothelial cells to stimulate angiogenesis. But that is not all this important factor does. VEGF has also controls

*Correspondence to: Prof. Dr. Ubaldo Armato, MD, Head, Histology and Embryology Unit, Department of Life and Reproduction Sciences, 8 Strada Le Grazie, I-37134 Verona, Italy. Tel./Fax: +39 045 8027159; E-mail: ubaldo.armato@univr.it.

ISSN 1387-2877/10/$27.50

neurogenesis in the sub-granular layer of adult dentate gyrus, and correspondingly, memory formation, the progressive failure of which is perhaps one of the most distressing characteristics of Alzheimer's disease (AD) [1].

A possible involvement of VEGF in AD is suggested by the *VEGF-A* gene being one of several genes upregulated, along with $A\beta_{1-42}$ accumulation in AD brains but not in age-matched normal brains [2,3]. Additionally, Kalaria and colleagues [4] found prominent immunoreactive VEGF in clusters of reactive astrocytes on blood vessel walls and in diffuse perivascular deposits of $A\beta_{1-42}$ in the neocortices of AD brains, but not in age-comparable normal brains. Because of this correlation between VEGF expression and AD, it is important to find out what causes astrocytes to synthesize VEGF, as this might have important consequences in an AD brain.

The VEGF expression in the AD brain could be caused by astrocytes reacting to local hypoxia, resulting from accumulation of perivascular $A\beta_{1-42}$, with the resulting stabilization of hypoxia-inducible factor (HIF)-1α protein and the nuclear translocation of HIF-1α · HIF-1β (ARNT1 or aryl hydrocarbon receptor nuclear translocator1) to stimulate *VEGF-A* gene expression. Alternatively accumulating $A\beta_{1-42}$ peptides might directly stimulate astrocytes independently of hypoxia to make VEGF. An $A\beta_{1-42}$-related action is suggested by the VEGF immunoreactivity in astrocytes and microglia and neovascularization that appear a week after injecting $A\beta_{1-42}$ into the normal rat hippocampus [5]. However, this week-long delay suggests that the injected $A\beta_{1-42}$ did not directly stimulate VEGF-A expression in the hippocampal glial cells – the VEGF expression required some $A\beta_{1-42}$-induced mediator(s). This could have been the proinflammatory cytokines that are well known to be produced by activated glial cells in the $A\beta_{1-42}$-accumulating AD brain [6,7].

Thus, the evidence for $A\beta_{1-42}$ being able to stimulate directly VEGF expression is equivocal. Park and Chae [8] have reported that $A\beta_{1-42}$ did not stimulate HN33 mouse neuroblastoma cells and neonatal rat astrocytes to make VEGF. On the other hand, Soucek and coworkers [9], working with cultured nerve cell lines and primary cortical neurons, reported that $A\beta_{1-42}$ stabilized HIF-1α, which in turn induced the formation of HIF1-α · HIF1-β, the heterodimeric transcription factor that stimulates the expression of the *VEGF-A* gene [10–18]. To resolve this contradictory issue, we have tested the VEGF-stimulating abilities of $A\beta_{25-35}$ and of proinflammatory cytokine(s) with a culture model that is directly relevant to the adult human brain; that is, phenotypically normal, proliferatively quiescent astrocytes from adult human temporal lobe cerebral cortex (NAHAs, normal adult human astrocytes). We will show that the synthetic peptide $A\beta_{25-35}$, an $A\beta_{1-42}$ surrogate whose physical and biological features it preserves [19] stabilizes HIF-1α protein without affecting HIF-1β expression and stimulates the nuclear translocation of the HIF-1α · HIF-1β heterodimer, its binding to HRE DNA, the expression of VEGF-A mRNA splice variants, and the secretion of VEGF-A_{165}, the major splice variant synthesized in NAHAs. We will also show that the mixture of three proinflammatory cytokines notoriously produced in AD brains, namely IL-1β+IFN-γ+TNF-α, which we have previously shown to strongly stimulate NAHAs to make nitric oxide (NO) [20–23], not only synergistically stabilizes HIF-1α protein but, unlike $A\beta_{25-35}$, also increases HIF-1β expression and consequently more strongly stimulates VEGF-A_{165} secretion.

MATERIALS AND METHODS

Isolation and culture of phenotypically normal NAHAs

NAHAs were isolated from temporal lobe cerebral cortex tissue fragments of five male patients (range: 18–38 years) with perforating head injuries due to motorcycle accidents who underwent neurosurgery immediately. The cells were promptly cultured and propagated as previously described in full detail [24–27]. The cells of these pure cultures only expressed astrocyte-specific markers such as glial fibrillary acid protein and glutamine synthase. None of the cells expressed neuronal (enolase), oligodendrocytes (galactocerebroside), microglia (CD-68), or endothelial cells (factor VIII) markers. These astrocytes proliferated slowly without added growth factors in 90% (v/v) Ham's F-12/MCDB 153 medium and 10% (v/v) heat-inactivated fetal bovine serum. They stopped growing upon reaching confluence. Under both proliferating and nonproliferating conditions the NAHAs steadily expressed their characteristic astrocyte markers – they were phenotypically "locked-in". But serum remained a necessary component of the medium and withdrawing it caused the astrocytes to self-destruct by apoptosis. The astrocytes of confluent, proliferatively quiescent cultures started cycling again when subcultured. Only astrocytes from the fourth to the eighth subculture were used because the response of the cells to proinflammatory cytokines or $A\beta_{25-35}$ became erratic with further subculturing.

Experimental protocol

Since astrocytes do not normally proliferate in the adult human brain, we studied the effects on VEGF-A production and release by Aβ_{25-35}, the reversed-sequence Aβ_{35-25} or proinflammatory cytokine(s) using confluent, proliferatively quiescent, pure NAHA cultures [24–27]. At "0-h", some cultures served as untreated controls, while others were treated with (i) 20 μM of either Aβ_{25-35} or the inactive Aβ_{35-25} (Bachem, Bubendorf, Switzerland) or (*ii*) IL-1β (20 ng ml), TNF-α (20 ng ml), and IFN-γ (70 ng ml) (all from PeproTech EC Ltd., London, UK) either administered individually or in pairs or as a three cytokine mixture (the CM-trio). These concentrations were previously shown to be non-cytotoxic and when administered together in a trio to potently stimulate MAP kinases and NO production in NAHAs [24–27]. Cultures were sampled between 18 h and 72 h after the onset of each treatment.

Expression of HIF-1α, HIF-1β (ARNT1), and VEGF-A splice variants' mRNAs assessed via RT-PCR

RNA was extracted using a total RNA extraction kit, Perfect Pure$^{\mathrm{TM}}$ (5PRIME, Eppendorf Italia, Milan, Italy), according to the manufacturer's instructions. The RNA quality was corroborated via electrophoresis of 1 μg of total RNA in 1% agarose gel 20 μg/ml ethidium bromide for 1 h at 90 V. Reverse transcription of 0.5 μg aliquots of total mRNA was carried out using the Transcriptor High Fidelity$^{\mathrm{TM}}$ cDNA Synthesis Sample Kit (Roche Diagnostics, Milan, Italy) according to the manufacturer's directions. Briefly, mRNA aliquots (0.5 μg) were mixed with 2.5 μg oligo (dT)-18 primers, heated for 10 min at 65°C and then cooled on ice. To the tube containing the template primer-mix, Transcriptor High Fidelity Reverse Transcriptase Reaction Buffer 1X 8 mM $MgCl_2$, 20 U Protector RNAse Inhibitor, deoxynucleotide mix 1 mM each, DTT 5 mM, 10 U Transcriptor High Fidelity Reverse Trascriptase were then added. The reaction was next incubated for 30 min at 45°C and for 5 min at 85°C. Specific primers for human VEGF-A and glyceraldehyde-3-phosphate dehydrogenase (GADPH) were those previously reported [28]. Specific primers for human HIF-1α and HIF-1β (ARNT1) were designed using Primer3 software (version 0.4.0 accessible in Internet) according to published sequences from the GenBank, that is: HIF-1α, 5'-CCGCTGGAGACACAATCATA-3' (sense) and 5'-GCTTGCGGAACTGCTTTC-TA-3' (antisense); HIF-1β, 5'-TGGTTTGGCAGCACACTCTA-3' (sense), and 5'-TCCATTCCTGCATCTGTTCC-3' (antisense). Each primer spanned at least an exon-intron boundary. The primers were made by Invitrogen (Paisley, UK). To obtain a linear amplification range, serial dilutions of cDNA preparations from NAHAs were PCR-amplified for 15–30 cycles and the resulting products run on a 2% agarose gel for 90 min at 90 V and stained by stirring with Syto®60 (Invitrogen) 1:20000 in RNAse-DNAse-free water for 45 min. Standard curves for each gene product were thus obtained. The PCR amplifications were processed with a DNA thermal cycler (MiniCycler$^{\mathrm{TM}}$, MJ Research, M-Medical S.r.l, Milan, Italy) in a final volume of 25 μl containing 2.5 mM $MgCl_2$, 1.5 U of HotMaster$^{\mathrm{TM}}$ *Taq* DNA polymerase (Eppendorf), 0.2 mM dNTPs, 0.4 μg of each primer, 1X reaction buffer, and 2 μl of cDNA per reaction. Thereafter, PCR amplifications were performed as follows: VEGF-A, through 26 cycles of 95°C for 30 s, 60°C for 1 min, and 72°C for 1 min; HIF-1α and GADPH, through 23 and 22 cycles, respectively, of 94°C for 30 s, 55°C for 1 min, and 72°C for 1 min; HIF-1β, through 25 cycles of 94°C for 30 s, 60°C for 10 s, and 72°C for 20 s. The final PCR products were electrophoresed on 2% agarose gel in 1X tris-borate EDTA buffer for 90 min at 90 V, stained by stirring with Syto®60 1:20000 in RNAse-DNAse-free water for 45 min, scanned in an Odissey$^{\mathrm{TM}}$ infrared imaging system (Licor Biosciences, Inc.; Lincoln, NE), and the integrated intensity of each specific band accurately quantified (in arbitrary units) using proprietary software. To permit semi-quantitative analysis GAPDH was utilized as an internal control. Sequencing analyses validated the identities of the PCR DNA products fragments (not shown).

Western immunoblotting

At chosen time points, control and treated NAHAs were scraped into cold PBS, sedimented at 200 g for 10 min, and homogenized in T-PER$^{\mathrm{TM}}$ tissue protein extraction reagent (Pierce, Rockford, IL) containing a complete EDTA-free protease inhibitor cocktail (Roche). The protein contents of the samples were determined according to Bradford [29] using BSA as standard. Equal amounts (10–20 μg) of protein from the samples were heat-denatured for 10 min at 70°C in an appropriate volume of 1X NuPAGE LDS Sample Buffer supplemented with 1X NuPAGE Reducing Agent (Invitrogen). The samples were next loaded on a NuPAGE Novex 10% Bis-Tris polyacrylamide gel

(Invitrogen). After electrophoresis in NuPAGE MOPS SDS Running Buffer using the Xcell SureLock^{TM} Mini-Cell (Invitrogen) (50 min run-time at 200 V constant), proteins were blotted onto nitrocellulose membranes (0.2 μm; Pall Italia, Milan, Italy). To ensure efficient and reproducible binding to the membrane, transfer proceeded under low power (30 V constant) for 1-h in 1X NuPAGE Transfer Buffer containing 10% methanol and 0.1% NuPAGE antioxidant. Membranes were probed with rabbit anti-human VEGF-A IgG polyclonal antibody (Santa Cruz Biotechnology; Heidelberg, Germany) or rabbit anti-HIF-1α antibody (Novus Biologicals, Littleton, CO) or anti-HIF-1β antibody (Santa Cruz Biotechnology) or anti-lamin B1 antibody (Santa Cruz Biotechnology) at a final dilution of 1 μg ml. Subsequent processing was carried out as previously detailed [24–27]. Lamin B1 was used as the loading control.

ELISA assay of VEGF-A

Cell-conditioned growth media were taken at 0-h, 18-h, 24-h, 48-h, and 72-h after the onset of exposure of NAHA cultures to each individual cytokine or cytokine pairs, CM-trio, or Aβ_{25-35} or Aβ_{35-25}, and stored at -80°C to be subsequently assayed for their VEGF-A content. This was done with a specific commercial ELISA kit (PeproTech). The tests were carried out according to the instructions of the manufacturer. The sensitivity of the assays for VEGF-A was 16 pg ml.

ELISA for HIF-1α transcriptional activity

NAHAs nuclear proteins were extracted using a kit from Panomics (Fremont, CA) and carried out as suggested by the manufacturer. Protein content was determined by the Bradford protein assay kit (Bio-Rad; Milan, Italy). An ELISA kit from Panomics was used to assess the hypoxia response element (HRE) DNA binding of the nuclear-extracted HIF-1α transcription factor. Briefly, to form the HIF-1α/HRE DNA complex, 40 μl of binding buffer master mix were incubated with 10 μl of sample nuclear extract (0.5 μg/ml) in the sample plates for 30 min at room temperature. From each well of the sample plate, 45 μl were then transferred to the assay plate. To capture the HIF-1α/HRE DNA complex, the assay plate was washed three times with the provided buffer and the samples were incubated with a primary antibody against HIF-1α for 1 h at room temperature. After washing and incubation with the secondary antibody, colorimetric signals were then developed by adding a TMB substrate solution to each well, and read with a Multiskan^{TM} (Labsystems, Finland) spectrophotometer at 450 nm.

Statistics

The data were analyzed using SigmaStat® 3.5 Advisory Statistics for Scientists (Systat Software, Richmond, CA). For RT-PCRs, data were normalized to GADPH and next analyzed by one-way ANOVA. For immunoblotting, data were normalized to lamin B1 and next analyzed by one-way ANOVA. *Post hoc* Holm-Sidak's test was used for multiple pair-wise comparisons. Null hypotheses were rejected when $P > 0.05$.

RESULTS

VEGF-A protein secreted into the NAHA-conditioned growth medium

We could detect small amounts of VEGF-A released into the medium by the untreated NAHAs (Fig. 1A,B). When administered separately, IL-1β, TNF-α, or IFN-γ did not significantly change the basal 72 h VEGF-A secretion ($P > 0.05$ vs. controls [None]) (Fig. 1A). Of the cytokine pairs tested only the TNF-α+IFN-γ could increase VEGF-A secretion ($P < 0.001$ vs. controls). However, the CM-trio (IL-1β+IFN-γ+TNF-α) was the strongest stimulator of VEGF-A secretion by 72 h ($P < 0.001$ or < 0.002 vs. controls and all other cytokine[s] treatments; Fig. 1A). Aβ_{25-35} by itself also significantly, though less strongly, stimulated VEGF-A secretion by 72 h ($P < 0.001$ vs. controls) (Fig. 1A). By contrast, the reverse-sequence Aβ peptide, Aβ_{35-25}, was ineffective ($P > 0.05$ vs. controls), which established the specificity of the stimulatory action of Aβ_{25-35} (Fig. 1A).

The timings of the VEGF responses to Aβ_{25-35} and the CM-trio are shown in Fig. 1B. The extracellular VEGF-A level stimulated by the CM-trio started rising after 18 h, and the level stimulated by Aβ_{25-35} started rising after 24 h and then both rose steadily thereafter (Fig. 1B). According to the areas under the three secretion curves in Fig. 1B, the *total* amount of VEGF-A secreted between 0 and 72 h by the CM-trio-stimulated NAHAs was 289% higher than the amount secreted by untreated cells and that by the Aβ_{25-35}-treated NAHAs was 148% higher than that secreted by untreated cells (in both instances $P < 0.05$ vs. untreated controls) (Table 1). Then again, the total amount of VEGF-A secreted by the CM-trio-treated NAHAs was 36% more than the amount secreted by the Aβ_{25-35}-treated NAHAs and this difference was significant ($P < 0.05$) (Table 1).

Table 1
Total 0-to-72-h VEGF-A secretion by cultured NAHAs

Treatment	Total VEGF-A secreted*	% Change	Levels of statistical significance**
None	566 ± 135	- - - -	- - - -
CM-trio	2203 ± 325	+ 289% vs. None	$P < 0.05$
Aβ_{25-35}	1406 ± 232	+ 148% vs. None − 36% vs. CM-trio	$P < 0.05$ $P < 0.05$

*Total VEGF-A secretion was obtained via the integral calculus of the surface areas (in mm^2) under the secretion curves in Fig. 1B. Points in the curves are expressed in pg ml^{-1} of the means ± SEM of the samples, each assayed in triplicate, from 25 untreated (None) cultures and 5–7 Aβ_{25-35}- or CM-trio-treated cultures. One-way ANOVA analysis of the complete data set provided an F value of 16.323 ($P < 0.001$).
**Pair-wise comparisons were carried out using *post-hoc* Holm-Sidak's test.

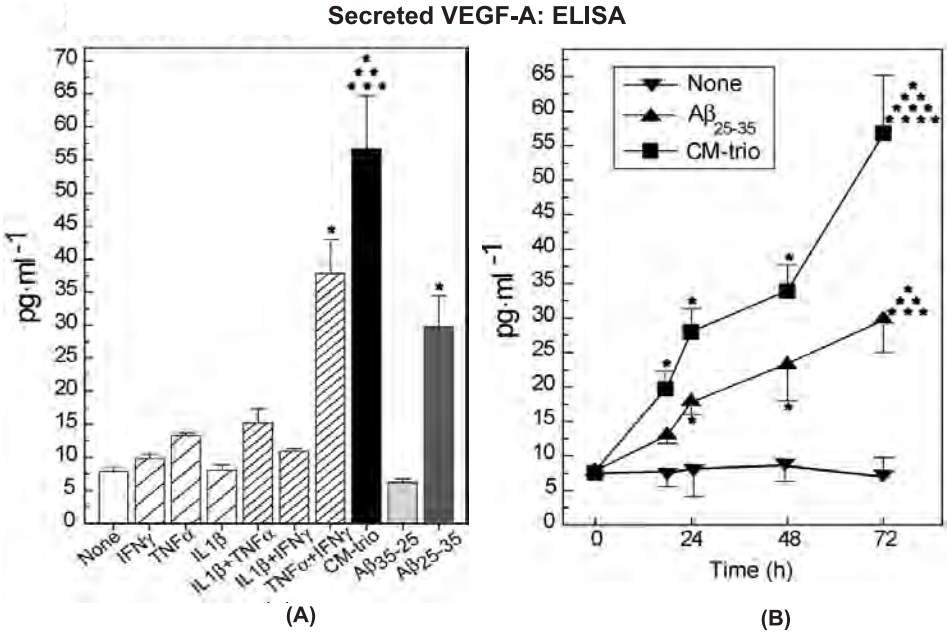

Fig. 1. (A) VEGF-A secretion from NAHAs was induced by Aβ_{25-35} by itself, by CM-trio, and by a TNF-α+IFN-γ pair, but not by any of the other cytokine treatments shown nor by the reversed-sequence peptide Aβ_{35-25}. Bars are the means ± SEMs of the values from 25 separate untreated (None) cultures, 12 Aβ_{25-35}-, 3 Aβ_{35-25}-, 7 CM-trio-, and 3 individual cytokines- or cytokine pairs-treated cultures, each assayed in triplicate. Analysis by ANOVA: $F = 21.035$, $P < 0.001$; pair-wise comparisons via *post-hoc* Holm-Sidak's test: $^{*}P < 0.001$ vs. None (untreated controls), individual and paired cytokines (save TNF-α+IFN-γ); $^{**}P < 0.001$ vs. TNF-α+IFN-γ; $^{***}P < 0.001$ vs. Aβ_{25-35}. (B) Time-related effects of CM-trio and of Aβ_{25-35} on VEGF-A secretion by NAHA cultures. Levels of statistical significance: ANOVA: None (untreated controls), F = 0.0795, $P > 0.05$; Aβ_{25-35}, $F = 14.132$, $P < 0.001$; CM-trio, F = 39.526, $P < 0.001$; pair-wise comparisons with *post hoc* Holm-Sidak's test, $^{*}P < 0.05$ vs. 0-h levels; $^{**}P < 0.05$ vs. 18-h levels; $^{***}P < 0.05$ vs. 24 h levels; $^{****}P < 0.05$ vs. 48 h levels. CM-trio-induced increases in secreted VEGF-A at both 24 h and 72 h were significantly higher (t test, $P < 0.05$) than the surges caused by Aβ_{25-35}. For the *total* 0-to-72-h secretion of VEGF-A by the NAHAs see Table 1.

Thus, VEGF-A secretion by NAHAs was strongly increased by either the CM-trio or Aβ_{25-35} experimental treatments, but we did not know what VEGF-A splice variants were secreted. To find this out we analyzed the proteins in NAHAs lysates via immunoblotting.

VEGF-A splice variants in NAHAs lysates

The NAHAs expressed three protein splice variants of VEGF-A, i.e., VEGF-A_{121}, VEGF-A_{165}, and VEGF-A_{189} (Fig. 2A). But, as expected, production of one of them, in this case VEGF-A_{165}, predominated. Indeed, to measure VEGF-A_{189} and VEGF-A_{121} in the immunoblots, it was necessary to load 4 to 5-fold more NAHAs' protein lysate than the usual 10–20 μg into the gel lanes. Since about three quarters of the total VEGF-A protein in the NAHAs lysates was VEGF-A_{165}, we focused our attention on it (Fig. 2A). Thus, our immunoblot studies showed that the intracellular VEGF-A_{165} protein level fell slightly but not

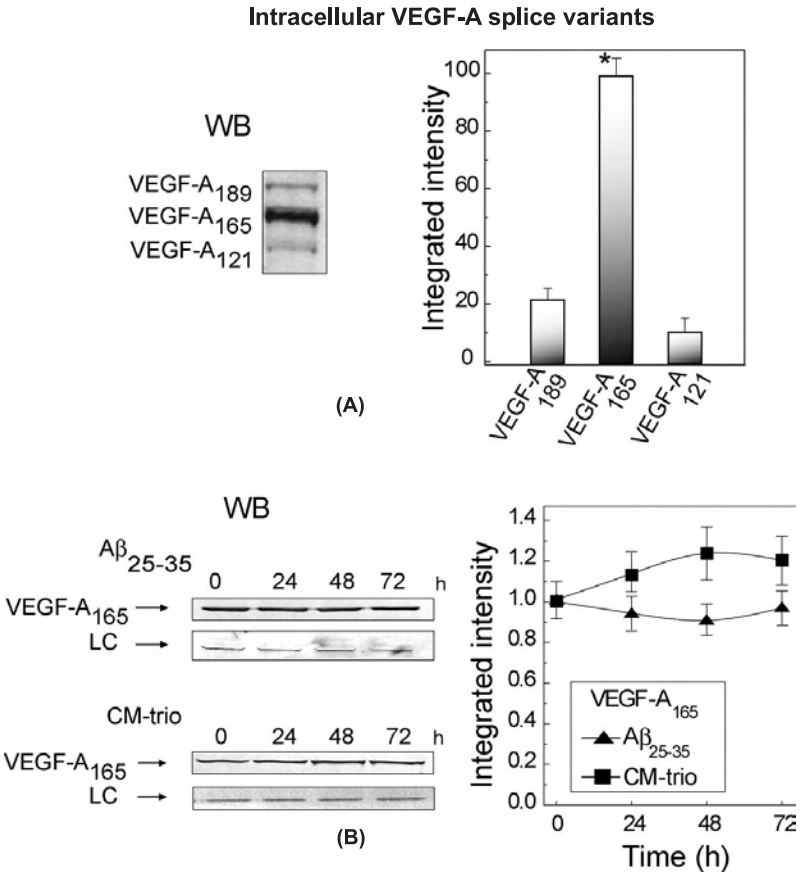

Fig. 2. VEGF-A_{165} was the predominant splice variant protein secreted by NAHAs into the medium but its *intracellular* levels were not significantly changed by exposure to the CM-trio or to Aβ_{25-35}. (A) *Left*, the predominant VEGF-A variant, VEGF-A_{165}, was readily detected in immunoblots, but VEGF-A_{189} and VEGF-A_{121}, were detectable only after loading with 4 to 5-fold more lysate proteins than usual. An immunoblot typical of those from 4 separate experiments is shown. *Right*, results of densitometric assessment of the integrated intensities (in arbitrary units) revealed that ∼75% of the VEGF-A protein was VEGF-A_{165}, on which we therefore focused our attention. Levels of statistical significance: ANOVA: $F = 86.048$, $P < 0.001$; pair-wise comparisons with *post hoc* Holm-Sidak's test, *, VEGF-A_{165} vs. VEGF-A_{189} or VEGF-A_{121}, $P < 0.05$; but VEGF-A_{189} vs. VEGF-A_{121}, $P > 0.05$. (B) *Left*, Western immunoblots (WB) were set up loading 10-20 μg of total protein lysates from untreated (0-h) or CM-trio- or Aβ_{25-35}-exposed NAHAs sampled according to the experimental protocol. LC, loading control (i.e., lamin B1). *Right*, results of corresponding densitometric evaluations of the VEGF-A_{165}-specific bands expressed as integrated intensities (in arbitrary units). Points in the curves are the means ± SEM of 5 experiments with 0-h values normalized to 1.0. No statistically significant differences vs. 0-h levels could be detected (ANOVA: Aβ_{25-35}, $F = 0.230$, $P > 0.05$; CM-trio, $F = 0.970$, $P > 0.05$).

significantly (−10% by 48 h vs. 0 h levels; $P > 0.05$) in Aβ_{25-35}-treated NAHAs, while it rose slightly, but again not significantly (+25% by 48 h vs. 0 h levels; $P > 0.05$) in CM-trio-treated NAHAs (Fig. 2B). Thus, nearly all of the newly produced VEGF-A_{165} was rapidly released by NAHAs into the medium and not significantly stored in the cytoplasm.

VEGF-A splice variant mRNAs in NAHAs

Alternative splicing of the *VEGF-A* RNA transcript at the gene's exons 6 and 7 is known to produce several different mRNAs [30,31]. As expected from the immunoblots, we found, using RT-PCR, that untreated NAHAs did indeed express three *VEGF-A* mRNA transcripts corresponding to the above mentioned three VEGF-A isoforms (Fig. 3).

We found in Aβ_{25-35}-exposed NAHAs that by 72 h the major VEGF-A_{165} and the minor VEGF-A_{189} mRNAs were significantly ($P < 0.05$) upregulated vs. basal (0 h) values, whereas the minor VEGF-A_{121}-encoding mRNA did not undergo statistically significant ($P > 0.05$) changes between 24 h and 72 h (Fig. 3A). In the CM-trio-exposed NAHAs, the levels of the VEGF-A_{189}, VEGF-A_{165}, and VEGF-A_{121} mRNAs were all significantly increased ($P < 0.05$) over

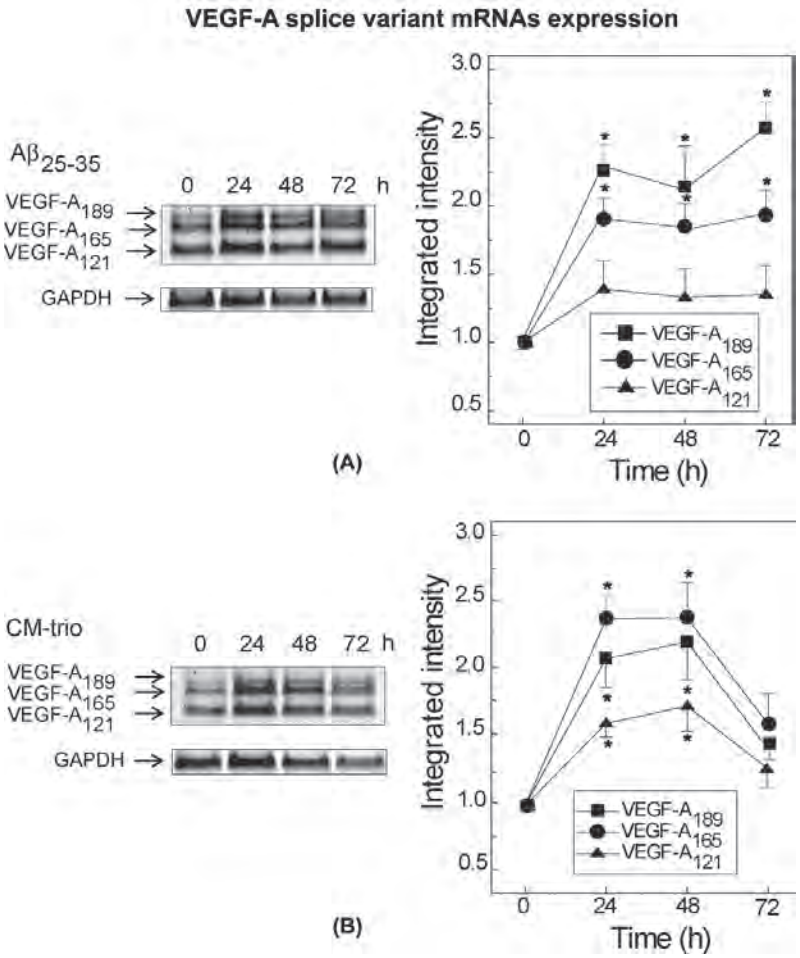

Fig. 3. An increased expression of the major VEGF-A_{165} and minor VEGF-A_{189} splice variant mRNAs was induced in either $A\beta_{25-35}$- or CM-trio-treated NAHAs. A) *Left*, typical RT-PCR of samples from untreated (0-h) and $A\beta_{25-35}$-treated NAHAs. *Right*, results of the semiquantitative densitometric analysis of RT-PCR bands using GAPDH as an internal control (in arbitrary units). Points on the curves are means $\pm$ SEMs of 4 separate experiments. Levels of statistical significance: ANOVA: VEGF-A_{189}, $F = 14.606$, $P = 0.001$; VEGF-A_{165}, $F = 12.432$, $P > 0.001$; VEGF-A_{121}, $F = 1.046$, $P > 0.05$; pair-wise comparisons with *post hoc* Holm-Sidak's test, $^*P < 0.05$ vs. 0-time values. B) *Left*, typical RT-PCR of samples from untreated (0-h) and CM-trio-treated NAHAs. *Right*, results of the semiquantitative densitometric analysis of RT-PCR bands using GAPDH as an internal control (in arbitrary units). Points on the curves are means $\pm$ SEMs of 4 separate experiments. Levels of statistical significance: ANOVA: VEGF-A_{189}, $F = 8.879$, $P < 0.001$; VEGF-A_{165}, $F = 4.212$, $P = 0.022$; VEGF-A_{121}, $F = 6.839$, $P = 0.004$; pair-wise comparisons with *post hoc* Holm-Sidak's test, $^*P < 0.05$ vs. corresponding 0-time values.

basal (0 h) levels between 24 h and 48 h to fall thereafter (Fig. 3B). Thus, both $A\beta_{25-35}$ and the CM-trio significantly stimulated the mRNA expression of the major splice variant, VEGF-A_{165}.

HIF-1α and HIF-1β (ARNT1) mRNA and protein expression in NAHAs

We then asked whether $A\beta_{25-35}$ and the CM-trio could stimulate VEGF-A_{165} like hypoxia by simply stabilizing HIF-1α and thus enabling the formation of HIF-1α · HIF-1β (ARNT1) transcription factor heterodimer [10–13,32,33] or did they stimulate the *HIF-1α* and/or *HIF-1β* gene or directly the *VEGF-A* gene.

Neither $A\beta_{25-35}$ nor the CM-trio significantly changed the basal HIF-1α (Fig. 4A) or HIF-1β mRNA levels (Fig. 5A) in the NAHAs. Although they did not affect the *HIF-1α* gene expression, they stimulated a significant surge of HIF-1α protein between 0 h and 48 h (Fig. 4B). However, the CM-trio, but not $A\beta_{25-35}$, also significantly increased the HIF-1β protein level in NAHAs at 24 h and 48 h (Fig. 5B). Thus, while $A\beta_{25-35}$ stabilized only the O_2-sensitive HIF-1α protein, the CM-trio stabilized and augmented the levels

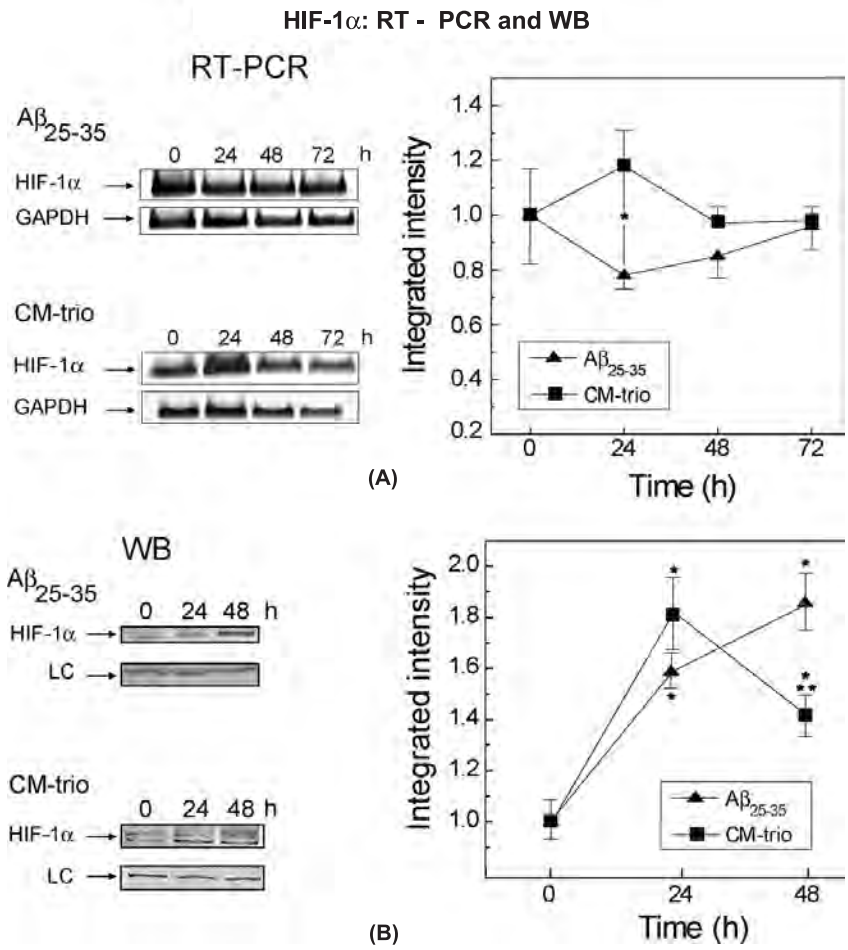

Fig. 4. HIF-1α mRNA expression did not increase, while HIF-1α protein levels significantly increased, in the CM-trio- or Aβ_{25-35}-treated NAHAs. A) *Left*, typical RT-PCRs of samples from untreated or CM-trio- or Aβ_{25-35}-treated NAHAs. *Right*, results of semiquantitative densitometric analysis of RT-PCR bands (using GAPDH as an internal control) expressed as integrated intensities (in arbitrary units). Points in the curves are the means $\pm$ SEM of 4 experiments with 0-time values normalized as 1.0. Levels of statistical significance: ANOVA: Aβ_{25-35}, $F = 0.767$, $P > 0.05$; CM-trio, $F = 0.757$, $P > 0.05$. However, the values of 24-h Aβ_{25-35} and 24-h CM-trio differed significantly from each other (t test, $^{*}P = 0.021$). B) *Left*, HIF-1α-specific protein bands in typical immunoblots (WB) of total protein lysates from untreated or CM-trio- or Aβ_{25-35}-treated NAHAs. LC, loading control (i.e., lamin B1). *Right*, results of densitometric appraisals of the integrated intensities (in arbitrary units) of the HIF-1α specific bands vs. 0-h values that were normalized to 1.0. Points in the curves are the normalized means $\pm$ SEM of the values from 5 distinct experiments. Levels of statistical significance: ANOVA: Aβ_{25-35}, $F = 22.796$, $P < 0.001$; CM-trio, $F = 12.897$, $P < 0.001$; pair-wise comparisons with *post hoc* Holm-Sidak's test, $^{*}P < 0.05$ vs. 0-time; $^{**}P < 0.05$ vs. corresponding 24-h value.

of both the HIF-1α and HIF-1β transcription factors in the 'normoxic' NAHAs.

HIF-1α nuclear translocation and DNA binding at HRE sites in NAHAs

We then found that Aβ_{25-35} or the CM-trio significantly stimulated the nuclear translocation and HRE DNA binding of the HIF-1α, and therefore the HIF-1α $\cdot$ HIF-1β heterodimer, in the NAHAs (Fig. 6). The nuclear HRE DNA-bound HIF-1α level peaked around 24 h with the Aβ_{25-35}-driven translocation being slightly slower than the CM-trio-driven translocation (Fig. 6). But then the nuclear levels of HIF-1α in both the Aβ_{25-35}- and CM-trio-treated NAHAs dropped rapidly to the starting level by 48 h. Thus, the reason for the CM-trio's superior ability to stimulate VEGF-A$_{165}$ production and secretion, as shown in Fig. 1, could consist in the ability of the CM-trio to stabilize and hence increase both HIF-1α and HIF-1β levels (Figs 4B and 5B) and, therefore, boost the flow of *VEGF-A* gene-activating HIF-1α $\cdot$ HIF-1β het-

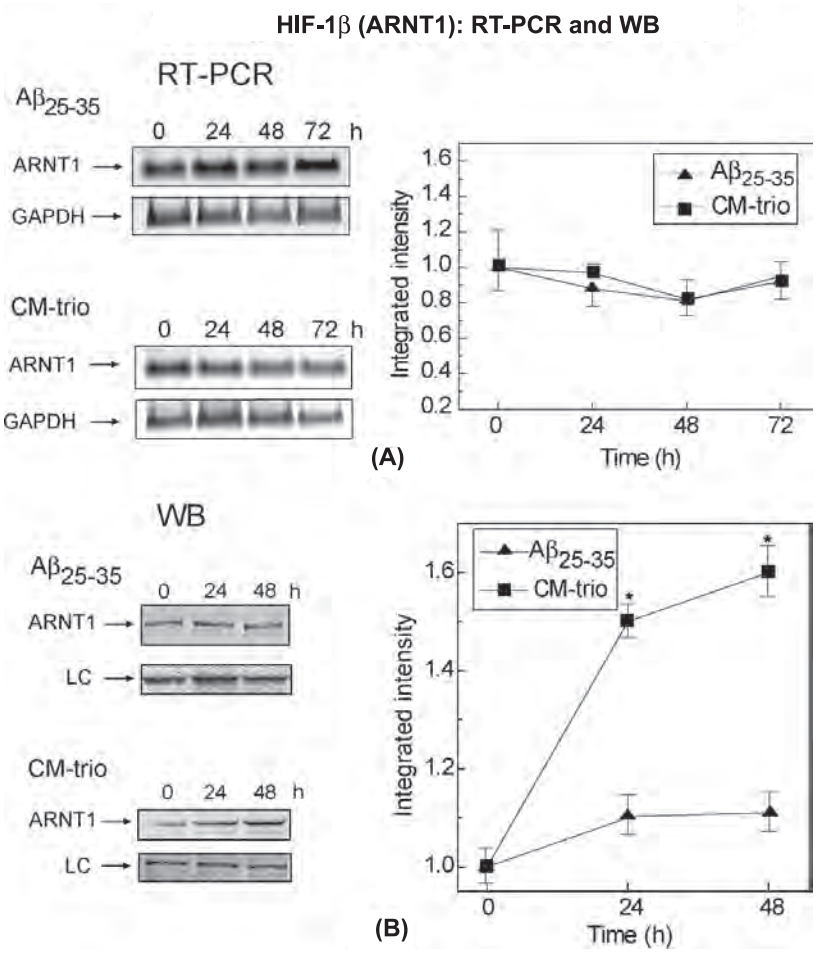

Fig. 5. HIF-1β (ARNT1) mRNA expression did not increase, while HIF-1β protein levels rose in CM-trio- but not in Aβ_{25-35}-treated NAHAs. A) *Left*, typical RT-PCRs of samples from untreated or CM-trio- or Aβ_{25-35}-treated NAHAs are shown. *Right*, results of semiquantitative densitometric analysis of specific RT-PCR bands using GAPDH as an internal control expressed as integrated intensities (in arbitrary units). Points in the curves are the means $\pm$ SEM of 4 experiments with 0-h values normalized as 1.0. Levels of statistical significance: ANOVA: Aβ_{25-35}, $F = 0.591$, $P > 0.05$; CM-trio, $F = 0.360$, $P > 0.05$. B) *Left*, HIF-1β (ARNT1)-specific protein bands in typical immunoblots (WB) set up with total NAHAs' protein lysates from untreated or CM-trio- or Aβ_{25-35}-treated NAHAs. LC, loading control (i.e., lamin B1). *Right*, results of densitometric assessment of the changes in intensity of HIF-1β-specific bands expressed as integrated intensities in arbitrary units vs. 0-h values that were normalized to 1.0. Points in the curves are the means $\pm$ SEMs of 5 separate experiments. Levels of statistical significance: ANOVA: Aβ_{25-35}, $F = 2.557$, $P > 0.05$; CM-trio, $F = 51.918$, $P < 0.001$; pair-wise comparisons with *post hoc* Holm-Sidak's test, $^*P < 0.05$ vs. corresponding 0-time values.

erodimers into the nucleus.

DISCUSSION

The present results obtained with relatively 'normoxic' NAHA cultures indicate that the VEGF-A production by astrocytes in AD brains, but not age-matched normal brains [6], need not be due just to hypoxia [4, 34–36], but also to the *direct* actions of Aβ peptides and the ensemble of cytokines accumulating in the inflammatory environment of these brains. Yet these agents acted like hypoxia by stimulating the formation and nuclear translocation of the HIF-1α · HIF-1β heterodimers. Surprisingly, unlike the Aβ_{1-42} surrogate Aβ_{25-35}, none of the three members of the cytokine trio could by itself significantly stimulate VEGF-A production by cultured NAHAs – they had to work together to induce the strongest stimulus of VEGF-A production and release. However, the TNF-α+IFN-γ pair did stimulate VEGF-A release, though less strongly than the trio. In previous work by Argaw et al. [37], a differ-

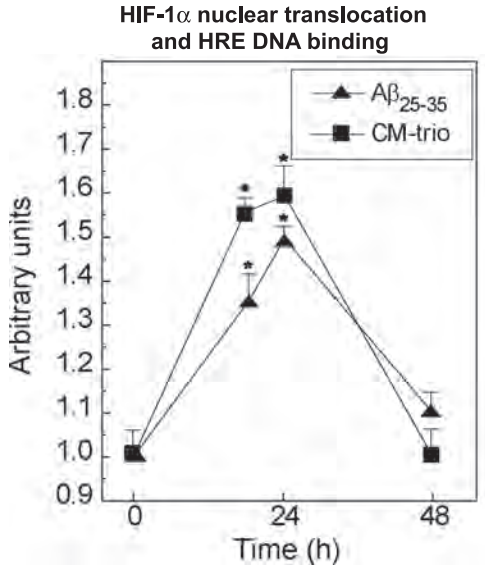

Fig. 6. The nuclear translocation and HRE DNA binding of HIF-1α protein was significantly increased in NAHAs exposed to either Aβ_{25-35} or the CM-trio. Points in the curves are the means $\pm$ SEM of 4 separate experiments with 0-h values normalized to 1.0. Levels of statistical significance: ANOVA: Aβ_{25-35}, $F = 15.902$, $P < 0.001$; CM-trio, $F = 28.903$, $P < 0.001$; pair-wise comparisons with*post hoc* Holm-Sidak's test, $^{*}P < 0.05$ vs. corresponding 0-time values.

ent cytokine pair, for example IL-1β+IFN-γ was found to stimulate VEGF-A secretion by normal *fetal* human astrocytes more efficiently than either IL-1β or IFN-γ given individually (the CM-trio was not tested). Even IL-1β by itself was a weaker yet effective stimulator in such cells. The divergence of our present findings from those of Argaw et al. [37] clearly implies that the modulation of VEGF-A production on the part of proinflammatory cytokines changes significantly as the normal fetal human astrocyte matures into an adult cell. Hence, caution should be advisable in extrapolating the cytokine-induced stimulatory mechanisms from fetal to adult human astrocytes.

Thus, both Aβ_{25-35} and the CM-trio did stimulate VEGF-A$_{165}$ transcript expression and increased the formation and nuclear translocation of HIF-1α $\cdot$ HIF-1β heterodimers. But the question arises as to how Aβ_{25-35} and the CM-trio could have stabilized HIF-1α to produce HIF-1α $\cdot$ HIF-1β heterodimers in our 'normoxic' NAHA cultures. One possibility might be the strong stimulation by the cytokine ensemble and by Aβ_{25-35} of the expression of the *NOS*-2 (NO synthase-2) gene and production of the proline hydroxylase-inhibiting NO [24,25,38,39]. This NO certainly would stabilize HIF-1α and enable HIF-1α $\cdot$ HIF-1β formation [40–43], but it happens too late [24,25]. Indeed, the nuclear translocation of HIF-1α $\cdot$ HIF-1β to the HRE DNA sites in the NAHAs peaked at 24 h, *not* 72 h, as did the NO production in NAHA cultures (data not shown; [24,25]). Clearly, it remains to be discovered how Aβ_{25-35} by itself and the synergistically acting members of the CM-trio stabilized HIF-1α in NAHAs. Nevertheless, our results obtained with the cultured NAHAs could explain the delayed VEGF response of rat hippocampal astrocytes to injected Aβ_{1-42} reported by Zand et al. [5] – they had to wait for the injected Aβ_{1-42} to induce microglia to generate an inflammatory environment and release an effective cytokine ensemble [7,20–23].

Finally, we should look at what an abnormal Aβ_{1-42}- and cytokines-driven VEGF-A production might do in the proinflammatory environment of an AD brain. The release of angiogenic VEGF-A from the astrocytes of the neurobarrier-coupling units with their blood vessel-attached end-feet [44,45] would be expected in an AD brain to produce new blood vessels to reverse or at least minimize the Aβ_{1-42}-induced vascular damage responsible for hypoxia, glucose shortages, breached blood-brain barrier and failing Aβ_{1-42} drainage [33, 46–51]. But it may not do so, because hypoxic endothelial cells in the hypoperfused regions of an AD brain downregulate their MEOX-2 homeobox gene and its GAX protein product [47,52]. This causes the endothelial cells to upregulate the AFX1 forkhead transcription factor that downregulates their anti-apoptogenesis Bcl-XL gene by stimulating the BCL-6 transcriptional repressor [52,53]. The downregulation of MEOX-2 homeobox gene and its GAX protein product also lowers the level of the Aβ_{1-42}-clearing soluble LRP1 [47, 52]. Therefore, while the increased VEGF production in an AD brain would indeed stimulate angiogenesis, this could counterproductively produce dysfunctional blood vessels with endothelial cells unable to clear Aβ_{1-42} and hyper-prone to apoptogenesis.

While VEGF-A is best known for its angiogenic action, it has only recently been found to operate as a major factor in the radial glial (astrocyte-like) cell/vascular-based stem cell niche in the sub-granular zone of the dentate gyrus [1,34]. There it links angiogenesis and vascular endothelial cell-produced brain-derived neurotrophic factor (BDNF) and BDNF-stimulated adult neurogenesis to continuously supply the new granular cells needed to start recording the memory of novel polymodal inputs from the entorhinal cortex [1,54]. Therefore, the increased expression of VEGF-A by astrocytes in a normal brain or induced

by Zand et al.'s [5] injection of $A\beta_{1-42}$ into rat brains might promote the survival and proliferation of neural progenitor cells, as indicated by the response of hippocampal neuronal progenitor cells to infusion of the protein into the lateral ventricles of adult rats [55]. But this may be unlikely in an AD brain with its elevated VEGF-A expression, as Waldau and Shetty [56] reported in their review of neural stem cells in AD brains that the AD pathology would prevent any VEGF-A-stimulated immature granule cells from differentiating into mature granule cells.

In conclusion, these observations suggest that the expression of VEGF by astrocytes that has been shown to occur in AD brains, but not normal aging brains, is likely because of the astrocytes responding to local hypoxia due vascular damage by accumulating perivascular $A\beta_{1-42}$, as well as to the direct actions of accumulating $A\beta_{1-42}$ and proinflammatory cytokines from activated microglia. The contribution of the VEGF to the development of AD remains to be shown, but we suggest that it is likely not trivial.

ACKNOWLEDGMENTS

The authors wish to thank Prof. A. Bricolo, Head, Neurosurgery Clinic, Major Hospital, Verona, Italy, and the Members of his Team for supplying the fragments of normal human adult temporal cortex, from which the astrocytes used in the present work were isolated. This work was supported in part by ex-60% Funds of the Italian MiUR (Ministry for University and Research) allotted to UA and AC.

Authors' disclosures available online (http://www.j-alz.com/disclosures/view.php?id=436).

REFERENCES

[1] Suh H, Deng W, Gage FH (2009) Signaling in adult neurogenesis. *Annu Rev Cell Dev Biol* **25**, 253-275.

[2] Pogue AI, Lukiw WJ (2004) Angiogenic signaling in Alzheimer's disease. *Neuroreport* **15**, 1507-1510.

[3] Thirumangalakudi L, Samany PG, Owoso A, Wiskar B, Grammas P (2006) Angiogenic proteins are expressed by brain blood vessels in Alzheimer's disease. *J Alzheimers Dis* **10**, 111-118.

[4] Kalaria RN, Cohen DL Premkumar DR, Nag S, LaManna JC, Lust WD (1998) Vascular endothelial growth factor in Alzheimer's disease and experimental cerebral ischemia. *Brain Res Mol Brain Res* **62**, 101-105.

[5] Zand L, Ryu JK, McLarnon JG (2005) Induction of angiogenesis in the beta-amyloid peptide-injected rat hippocampus. *Neuroreport* **16**, 129-132.

[6] Frede S, Berchner-Pfannschmidt U, Fandrey J (2007) Regulation of hypoxia-inducible factors during inflammation. *Methods Enzymol* **435**, 405-419.

[7] Ryu JK, McLarmon JG (2009) A leaky blood-brain barrier, fibrinogen infiltration and microglial reactivity in inflamed Alzheimer's disease brain. *J Cell Mol Med Jul* **13**, 2911-2925.

[8] Park SY, Chae CB (2007) Toxic levels of amyloid beta peptide do not induce VEGF synthesis. *Mol Cells* **24**, 69-75.

[9] Soucek T, Cumming R, Dargusch R, Maher P, Schubert D (2003) The regulation of glucose metabolism by HIF-1 mediates a neuroprotective response to amyloid beta peptide. *Neuron* **39**, 43-56.

[10] Brahimi-Horn MC, Pouysségur J (2007) Oxygen, a source of life and stress. *FEBS Lett* **581**, 3582-3591.

[11] Forsythe JA, Jiang BH, Iyer NV, Agani F, Leung SW, Koos RD, Semenza GL (1996) Activation of vascular endothelial growth factor gene transcription by hypoxia-inducible factor 1. *Mol Cell Biol* **16**, 4604-4613.

[12] Huang LE, Bunn HF (2003) O_2 sensing, HIF, and regulation of gene expression. *J Biol Chem* **278**, 19575-78.

[13] Ke Q, Costa M (2006) Hypoxia-inducible factor-1 (HIF-1). *Mol Pharmacol* **70**, 1469-1480.

[14] Koh MY, Darnay BG, Powis G (2008) Hypoxia-associated factor, a novel E3-ubiquitin ligase, binds and ubiquitinates hypoxia-inducible factor-1α, leading to its oxygen-independent degradation. *Mol Cell Biol* **28**, 7081-7095.

[15] Pagés G, Pouysségur J (2005) Transcriptional regulation of the vascular endothelial growth factor gene – a concert of activating factors. *Cardiovasc Res* **65**, 564-573.

[16] Ruiz de Almodovar C, Lambrechts D, Mazzone M, Carmeliet P (2009) Role and therapeutic potential of VEGF in the nervous system. *Physiol Rev* **89**, 607-648.

[17] Semenza GL (1999) Regulation of mammalian O_2 homeostasis by hypoxia-inducible factor 1. *Annu Rev Cell Dev Biol* **15**, 551-578.

[18] Semenza GL (2002) Signal transduction to hypoxia-inducible factor 1. *Biochem Pharmacol* **64**, 993-998.

[19] Kaminsky YG, Marlatt MW, Smith MA, Kosenko EA (2010) Subcellular and metabolic examination of amyloid-beta peptides in Alzheimer disease pathogenesis: evidence for Abeta(25–35). *Exp Neurol* **221**, 26-37.

[20] Dehne N, Brüne B (2009) HIF-1 in the inflammatory microenvironment. *Exp Cell Res* **315**, 1791-1797.

[21] Rogers J, Cooper NR, Webster S, Schultz J, McGeer PL, Styres SD, Civin WH, Brachova L, Bradt B, Ward P, Lieberburg I (1992) Complement activation by beta amyloid in Alzheimer's disease. *Proc Natl Acad Sci U S A* **89**, 10016-10020.

[22] McLarnon JG, Ryu JK (2008) Relevance of $A\beta_{1-42}$ intrahippocampal injection as an animal model of inflamed Alzheimer's disease brain. *Curr Alzheimer Res* **5**, 475-480.

[23] Ryu JK, Cho T, Choi HB, Wang YT, McLarnon JG (2009) Microglial VEGF receptor response is an integral chemotactic component in Alzheimer's disease pathology. *J Neurosci* **29**, 3-13.

[24] Chiarini A, Dal Pra I, Gottardo R, Bortolotti F, Whitfield JF, Armato U (2005) BH_4 (tetrahydrobiopterin)-dependent activation, but not the expression, of inducible NOS (nitric oxide synthase)-2 in proinflammatory cytokine-stimulated, cultured normal human astrocytes is mediated by MEK-ERK kinases. *J Cell Biochem* **94**,731-743.

[25] Chiarini A, Dal Pra I, Menapace L, Pacchiana R, Whitfield JF, Armato U (2005) Soluble amyloid beta peptide and myelin basic protein strongly stimulate, alone and in synergism with combined proinflammatory cytokines, the expression of func-

tional nitric oxide synthase-2 in normal adult human astrocytes. *Int J Mol Med* **16**, 801-807.

[26] Dal Pra I, Chiarini A, Nemeth EF, Armato U, Whitfield JF (2005) Roles of Ca^{2+} and the Ca^{2+}- sensing receptor (CASR) in the expression of inducible NOS (nitric oxide synthase)-2 and its BH_4 (tetrahydrobiopterin)-dependent activation in cytokine-stimulated adult human astrocytes. *J Cell Biochem* **96**, 428-438

[27] Chiarini A, Armato U, Pacchiana R, Dal Pra I (2009) Proteomic analysis of GTP cyclohydrolase 1 multiprotein complexes in cultured normal adult human astrocytes under both basal and cytokine-activated conditions. *Proteomics* **9**, 1850-1860.

[28] Bausero P, Ben-Mahdi M, Mazucatelli J, Bloy C, Perrot-Applanat M (2000) Vascular endothelial growth factor is modulated in vascular muscle cells by estradiol, tamoxifen, and hypoxia. *Am J Physiol Heart Circ Physiol* **279**, H2033-H2042.

[29] Bradford MM (1976) A rapid and sensitive method for the quantitation of microgram quantities protein utilizing the principle of protein-dye binding. *Anal Biochem* **72**, 248-254.

[30] Houck KA, Ferrara N, Winer J, Cachianes G, Li B, Leung DW (1991). The vascular endothelial growth factor family: identification of a fourth molecular species and characterization of alternative splicing of RNA. *Mol Endocrinol* **5**, 1806-1814.

[31] Whittle C, Gillespie K, Harrison R, Mathieson PW, Harper SJ (1999) Heterogeneous vascular endothelial growth factor (VEGF) isoform mRNA and receptor mRNA expression in human glomeruli, and the identification of $VEGF_{148}$ mRNA, a novel truncated splice variant. *Clin Sci* (Lond) **97**, 303-312.

[32] Semenza GL (2003) Angiogenesis in ischemic and neoplastic disorders. *Annu Rev Med* **54**, 17- 28.

[33] Schubert D, Soucek T, Blouw B (2009) The induction of HIF-1 reduces astrocyte activation by amyloid beta peptide. *Eur J Neurosci* **29**, 1323-1334.

[34] Carmeliet P, (2003) Blood vessels and nerves: common signals, pathways and diseases. *Nat Rev Genet* **4**, 710-20.

[35] Kalaria RN (1997) Cerebrovascular degeneration is related to amyloid beta protein deposition in Alzheimer's disease. *Ann N Y Acad Sci* **826**, 263-271.

[36] Kalaria RN (2002) Small vessel disease and Alzheimer's dementia: pathological considerations. *Cerebrovasc Dis* **13**, 48-52.

[37] Argaw AT, Zhang Y, Snyder BJ, Zhao ML, Kopp N, Lee SC, Raine CS, Brosman CF, John GR (2006) IL-1β regulates blood-brain barrier permeability via reactivation of the hypoxia-angiogenesis program. *J Immunol* **177**, 5574-5584.

[38] Chiarini A, Dal Pra I, Whitfield JF, Armato U (2006) The killing of neurons by beta-amyloid peptides, prions, and proinflammatory cytokines. *Ital J Anat Embryol* **111**, 221-246.

[39] Dal Pra I, Chiarini A, Pacchiana R, Chakravarthy B, Whitfield JF, Armato U (2008) Emerging concepts of how β-amyloid proteins and proinflammatory cytokines might collaborate to produce an 'Alzheimer brain'. *Mol Med Rep* **1**, 173-178.

[40] Brüne B, Zhou J (2007) Hypoxia-inducible factor-1α under the control of nitric oxide. *Methods Enzymol* **435**, 463-478.

[41] Kasuno K, Takabuchi S, Fukuda K, Kizaka-Kondoh S, Yodoi J, Adachi T, Semenza GL, Hirota K (2004) Nitric oxide induces hypoxia-inducible factor-1 activation that is dependent on MAPK and phosphatidylinositol 3-kinase signaling. *J Biol Chem* **279**, 2550-2558.

[42] Kimura H, Weisz A, Kurashima Y, Hashimoto K, Ogura T, D'Acquisto F, Addeo R, Makuuchi M, Esumi H (2000) Hypoxia response element of the human vascular endothelial growth factor gene mediates transcriptional regulation by nitric oxide: control of hypoxia-inducible factor-1 activity by nitric oxide. *Blood* **95**, 189-197.

[43] Kimura H, Weisz A, Ogura T, Hitomi Y, Kurashima Y, Hashimoto K, D'Acquisto F, Makuuchi M, Esumi H (2001) Identification of hypoxia-inducible factor 1 ancillary sequence and its function in vascular endothelial growth factor gene induction by hypoxia and nitric oxide. *J Biol Chem* **276**, 2292-2298.

[44] Jakovcevic D and Harder DR (2007) Role of astrocytes in matching blood flow to neuronal activity. *Curr Top Dev Biol* **79**, 75-97.

[45] Leybaert L, De Bock M, Van Moorhem M, Decrock E, De Vuyst E (2007) Neurobarrier coupling in the brain: adjusting glucose entry with demand. *J Neurosci Res* **85**, 3213-3220.

[46] Bell RD, Zlokovic BV (2009) Neurovascular mechanisms and blood-brain barrier disorder in Alzheimer's disease. *Acta Neuropathol* **118**, 103-113.

[47] Zlokovic BV (2008) The blood-brain barrier in health and chronic neurodegenerative disorders. *Neuron* **57**, 178-201.

[48] Farkas E, Luiten PG (2001) Cerebral microvascular pathology in aging and Alzheimer's disease. *Prog Neurobiol* **64**, 575-611.

[49] Stopa EG, Butala P, Salloway S, Johanson CE, Gonzalez L, Tavares R, Hovanesian V, Hulette CM, Vitek MP, Cohen RA (2008) Cerebral cortical arteriolar angiopathy, vascular β-amyloid, smooth muscle actin, Braak stage, and APOE genotype. *Stroke* **39**, 814-821.

[50] Thal DR, Griffin WS, Braak H (2008) Parenchymal and vascular Aβ-deposition and its effects on the degeneration of neurons and cognition in Alzheimer's disease. *J Cell Mol Med* **12**, 1848-1862.

[51] Zachary I (2005) Neuroprotective role of vascular endothelial growth factor: signalling mechanisms, biological function, and therapeutic potential. *Neurosignals* **14**, 207-221.

[52] Wu X, Jelinek DF (2005) A-Miz-ing BCL6. *Nat Immunol* **6**, 964-966.

[53] Tang TT, Dowbenko D, Jackson A, Toney L, Lewin DA, Dent AL, Lasky LA (2002) The forkhead transcription factor AFX activates apoptosis by induction of the BCL-6 transcriptional repressor. *J Biol Chem* **277**, 14255-14265.

[54] Whitfield JF, Chakravarthy BK (2009) The neuronal primary cilium: driver of neurogenesis and memory formation in the hippocampal dentate gyrus? *Cell Signal* **21**, 1351-1355.

[55] Schänzer A, Wachs FP, Wilhelm D, Acker T, Cooper-Kuhn C, Beck H, Winkler J, Aigner L, Plate KH, Kuhn HG (2004) Direct stimulation of adult neural stem cells *in vitro* and neurogenesis *in vivo* by vascular endothelial growth factor. *Brain Pathol* **14**, 237-248.

[56] Waldau B, Shetty AK. Behavior of neural stem cells in the Alzheimer brain. (2008) *Cell Mol Life Sci* **65**, 2372-2384.